Crescent States in Charge-Imbalanced Polariton Condensates

Artem Strashko,[1] Francesca M. Marchetti,[2] Allan H. MacDonald,[3] and Jonathan Keeling[4]
[1]Center for Computational Quantum Physics, Flatiron Institute, 162 5th Avenue, New York, New York 10010, USA
[2]Departamento de Fisica Teorica de la Materia Condensada & Condensed Matter Physics Center (IFIMAC), Universidad Autonoma de Madrid, Madrid 28049, Spain
[3]Department of Physics, University of Texas, Austin, Texas 78712, USA
[4]SUPA, School of Physics and Astronomy, University of St Andrews, St Andrews KY16 9SS, United Kingdom

(Received 3 February 2020; accepted 5 July 2020; published 7 August 2020)

We study two-dimensional charge-imbalanced electron-hole systems embedded in an optical microcavity. We find that strong coupling to photons favors states with pairing at zero or small center-of-mass momentum, leading to a condensed state with spontaneously broken time-reversal and rotational symmetry and unpaired carriers that occupy an anisotropic crescent-shaped sliver of momentum space. The crescent state is favored at moderate charge imbalance, while a Fulde–Ferrel–Larkin–Ovchinnikov-like state—with pairing at large center-of-mass momentum—occurs instead at strong imbalance. The crescent state stability results from long-range Coulomb interactions in combination with extremely long-range photon-mediated interactions.

DOI: 10.1103/PhysRevLett.125.067405

Introduction.—At low carrier densities, electrons and holes in two-dimensional (2D) semiconductors pair into bosonic excitons that can condense at low enough temperatures [1–5]. Exciton condensation is expected to survive the frustration of unequal electron and hole densities [6–11], which favors condensed electron-hole pairs that acquire a finite center-of-mass momentum forming a state similar to the Fulde–Ferrel [12] (FF) and Larkin–Ovchinnikov [13] (LO) phases (abbreviated as FFLO) known from superconductors. The prospect of FFLO phases has also been extensively discussed in the context of cold atoms [14]. Although FFLO phases are common to imbalanced two-component fermions with attractive interactions, more exotic alternatives, such as phase separation in momentum space (also named "breached pair" or "Sarma" phases), have been suggested in special cases [15,16]. In neutral systems, these uniform density imbalanced phases compete with, and are largely replaced by, phase separation in real space [17–19]. For the charged electron-hole systems we focus on here, however, the electrostatic energy forbids phase separation and exotic uniform states are a stronger possibility.

The Bose-Einstein condensation (BEC) temperature increases significantly when optically pumped 2D semiconductors are placed in a planar microcavity, designed so that long-wavelength confined photons are close to resonance with excitons [20,21]. The resulting quasiparticles, exciton-polaritons, are photon-exciton hybrids with greatly reduced mass [22]. This favors long-range coherence and yields more robust condensates than without a cavity [23]. In this Letter, we examine the influence of a resonant planar microcavity on condensation phenomena in 2D semiconductor structures with unequal electron and hole densities

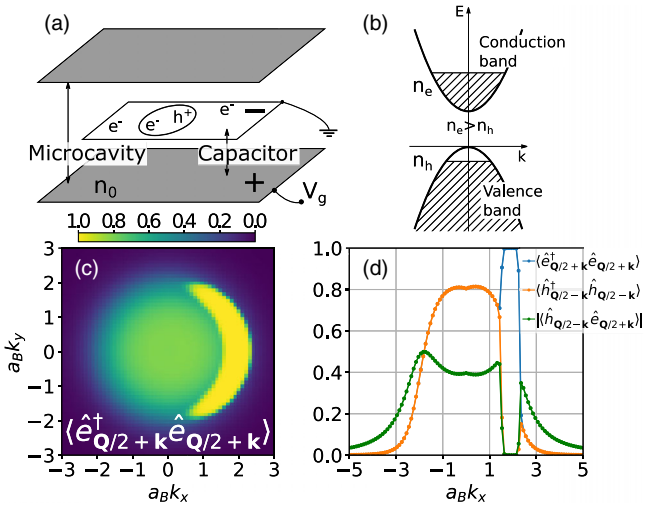

FIG. 1. (a) Semiconductor quantum well embedded in a planar microcavity with net charge tuned by a gate voltage between the bottom mirror and the grounded semiconductor. (b) Occupied bands with finite excitation and charge. (c) Typical anisotropic crescent state represented by the electron occupation. This occupation reaches one at low temperatures inside the yellow crescent-shaped region. (d) $k_y = 0$ momentum space slice of (c) showing both occupations and electron-hole coherence. Inside the Fermi surface [yellow in (c)], both conduction and valence bands are occupied so coherence vanishes. Elsewhere only one state is occupied. Parameters (as described in the text) are target charge density $n_0 = 8.125 \times 10^{-2} a_B^{-2}$, excitation chemical potential $\mu_{ex} = E_G + E_B$, temperature $k_B T = 0.04 E_B$, photon cutoff frequency $\omega_0 = 3.06 E_B$, matter-light coupling momentum cutoff $\kappa = 2.5 a_B^{-1}$, matter-light coupling $g_0 = 0.8 E_B a_B$, mass ratio $m_e/m_h = 1$, $\varepsilon = 1$, and capacitive energy $\alpha = 800 E_B a_B^2$.

[see Figs. 1(a) and (b)]. We find strong matter-light coupling favors small pairing-momentum states over FFLO states with larger pairing momentum. Specifically it induces breached pair states and anisotropic crescent states, explained below, which spontaneously break both rotational and time-reversal symmetry. The anisotropic states place excess carriers in a compact crescent-shaped sliver in momentum space on the edge of the region occupied by electron-hole pairs, as shown in Figs. 1(c) and (d). Crescent states were in fact considered as a potential state for small pairing wave vector [12,24] but, as shown in Ref. [24], are not the ground state of the superconducting problem. The crescent and breached pair states are stabilized only because of the coupling to light and the small photon mass. Further, as discussed later, the anisotropy also requires long-range Coulomb interactions. As such, while the electron-hole-photon model we will introduce below is superficially similar to the two-channel model of ultracold fermionic atoms [25], there are crucial differences. For atoms, interactions are contactlike and, most importantly, the analogue of the photon is a "closed channel" molecule with a mass twice that of the atoms. In addition, phase separation in real space dominates the phase diagram of cold atoms [17–19]. The states we propose here are thus unique to polaritons. These states can be identified experimentally by strongly anisotropic electrical transport that can be reoriented by altering the polariton-confinement landscapes or by weak resonant optical excitation. In the following we first explain the calculations that predict the crescent states and then discuss properties that could identify them experimentally.

Model.—We consider a model of electrons and holes, confined in 2D quantum wells, subject to Coulomb interactions, and coupled to cavity photons. The Hamiltonian is thus ($\hbar = 1$, $4\pi\varepsilon_0 = 1$):

$$\begin{aligned}\hat{H} = &\sum_{\mathbf{k}}\left[\left(\frac{k^2}{2m_e}+E_G\right)\hat{e}^\dagger_{\mathbf{k}}\hat{e}_{\mathbf{k}}+\frac{k^2}{2m_h}\hat{h}^\dagger_{\mathbf{k}}\hat{h}_{\mathbf{k}}\right]\\ &+\frac{1}{2S}\sum_{\mathbf{k},\mathbf{k}',\mathbf{p}}V_{\mathbf{p}}\{\hat{e}^\dagger_{\mathbf{k}+\mathbf{p}}\hat{e}^\dagger_{\mathbf{k}'-\mathbf{p}}\hat{e}_{\mathbf{k}'}\hat{e}_{\mathbf{k}}+\hat{h}^\dagger_{\mathbf{k}+\mathbf{p}}\hat{h}^\dagger_{\mathbf{k}'-\mathbf{p}}\hat{h}_{\mathbf{k}'}\hat{h}_{\mathbf{k}}\\ &-2\hat{e}^\dagger_{\mathbf{k}+\mathbf{p}}\hat{h}^\dagger_{\mathbf{k}'-\mathbf{p}}\hat{h}_{\mathbf{k}'}\hat{e}_{\mathbf{k}}\}+\alpha S(\hat{n}_c-n_0)^2\\ &+\sum_{\mathbf{k}}\omega_{\mathbf{k}}\hat{a}^\dagger_{\mathbf{k}}\hat{a}_{\mathbf{k}}+\sum_{\mathbf{k},\mathbf{p}}\frac{g_{\mathbf{k}}}{\sqrt{S}}(\hat{e}^\dagger_{\mathbf{k}}\hat{h}^\dagger_{\mathbf{p}-\mathbf{k}}\hat{a}_{\mathbf{p}}+\hat{a}^\dagger_{\mathbf{p}}\hat{h}_{\mathbf{p}-\mathbf{k}}\hat{e}_{\mathbf{k}}),\end{aligned}\quad(1)$$

where S is the system area. The first term in $\hat{H}$ describes noninteracting electrons and holes with masses m_e and m_h in a 2D semiconductor with band gap E_G. The second term is the mutual Coulomb interaction $V_{\mathbf{p}} = 2\pi e^2/\varepsilon p$, while the third term gives the dependence of the electrostatic energy on the system charge density. Here $\alpha = e^2 S/2C$ is an (intensive) capacitive scale that depends on the gating geometry. The target charge density, n_0, is proportional to a tunable gate voltage. Typically α is large compared to the corresponding interaction scale ($e^2 n_e^{-1/2}/\varepsilon$) so that the actual charge imbalance that minimizes the free energy is nearly identical to the target charge density, i.e., $\langle \hat{n}_c \rangle \simeq n_0$, where

$$\hat{n}_c = \frac{1}{S}\sum_{\mathbf{k}}(\hat{e}^\dagger_{\mathbf{k}}\hat{e}_{\mathbf{k}}-\hat{h}^\dagger_{\mathbf{k}}\hat{h}_{\mathbf{k}}) = \hat{n}_e - \hat{n}_h. \quad(2)$$

Including the electrostatic energy realistically, as we do in Eq. (1), allows us to use the grand canonical ensemble without generating unphysical phase separations and so enables us to consider more general variational ansatz states. The final line of Eq. (1) accounts for the photons and their coupling to matter. We assume a single branch of cavity photons with a quadratic dispersion, $\omega_{\mathbf{k}} = \omega_0 + k^2/2m_{\mathrm{ph}}$, where $m_{\mathrm{ph}} \simeq 10^{-4} m_e$. In the following we measure lengths in units of the 2D exciton Bohr radius $a_{\mathrm{B}} = \varepsilon/(2\mu e^2)$, where $\mu = m_e m_h/(m_e + m_h)$, and energies in units of $E_{\mathrm{B}} = 1/(2\mu a_{\mathrm{B}}^2)$.

To avoid the ultraviolet divergences produced by a momentum-independent matter-light coupling [26–30], we take $g_{\mathbf{k}} = g_0 e^{-|\mathbf{k}|/\kappa}$ and choose $1/\kappa$ to be of the order of the material lattice constant. This cutoff breaks the theory gauge invariance under the replacement $\hat{e}_{\mathbf{k}} \to \hat{e}_{\mathbf{k}+e\mathbf{A}}, \hat{h}_{\mathbf{k}} \to \hat{h}_{\mathbf{k}-e\mathbf{A}}$, which could be recovered by taking $\kappa \to \infty$ and renormalizing the photon frequency (see Refs. [30,31]). Full gauge invariance requires consistency of the band and matter-light coupling Hamiltonians [33] and is crucial to recover the no-go theorems precluding ground state superradiance [33,34].

To control the excitation density we introduce a chemical potential, μ_{ex}, and replace $\hat{H} \to \hat{H} - S\mu_{\mathrm{ex}}\hat{n}_{\mathrm{ex}}$, where

$$\hat{n}_{\mathrm{ex}} = \frac{1}{S}\sum_{\mathbf{k}}\left[\hat{a}^\dagger_{\mathbf{k}}\hat{a}_{\mathbf{k}}+\frac{1}{2}(\hat{e}^\dagger_{\mathbf{k}}\hat{e}_{\mathbf{k}}+\hat{h}^\dagger_{\mathbf{k}}\hat{h}_{\mathbf{k}})\right]. \quad(3)$$

The energy shift accounts for the time dependence of the nonequilibrium condensates that form at finite excitation density. The no-go theorem does not apply for a system at finite excitation density [35]. We note that, because we make the rotating wave approximation, equal shifts in ω_0, E_G, and μ_{ex} have no effect.

Variational approach.—To estimate the *finite temperature* phase diagram of our model, we use a variational ansatz for the density matrix [36], $\hat{\rho}_v = \exp(-\beta\hat{H}_v)/\mathcal{Z}_v$, $\mathcal{Z}_v = \mathrm{Tr}[\exp(-\beta\hat{H}_v)]$. We then minimize the free energy corresponding to this density matrix, $F_v = \langle\hat{H}\rangle_v + k_B T \mathrm{Tr}[\hat{\rho}_v \ln\hat{\rho}_v] = \langle\hat{H}-\hat{H}_v\rangle_v - k_B T \ln\mathcal{Z}_v$, where $\langle\hat{X}\rangle_v = \mathrm{Tr}(\hat{\rho}_v\hat{X})$. Standard thermodynamic identities allow one to show that F_v is an upper bound on the true free energy. The variational Hamiltonian $\hat{H}_v$ should be chosen to be solvable, and for our model, we should allow for electron-hole coherence, photon coherence, population imbalance, and

arbitrary polariton momentum $\mathbf{Q}$. We therefore consider a variational Hamiltonian of the form

$$\hat{H}_v = \nu_{\mathbf{Q}}\sqrt{S}\phi(\hat{a}^\dagger_{\mathbf{Q}} + \hat{a}_{\mathbf{Q}}) + \sum_{\mathbf{q}} \nu_{\mathbf{q}} \hat{a}^\dagger_{\mathbf{q}} \hat{a}_{\mathbf{q}} + \sum_{\mathbf{k}} \begin{pmatrix} \hat{e}^\dagger_{\frac{\mathbf{Q}}{2}+\mathbf{k}} & \hat{h}_{\frac{\mathbf{Q}}{2}-\mathbf{k}} \end{pmatrix} \begin{pmatrix} \eta^e_{\mathbf{k}} & \Delta_{\mathbf{k}} \\ \Delta_{\mathbf{k}} & -\eta^h_{\mathbf{k}} \end{pmatrix} \begin{pmatrix} \hat{e}_{\frac{\mathbf{Q}}{2}+\mathbf{k}} \\ \hat{h}^\dagger_{\frac{\mathbf{Q}}{2}-\mathbf{k}} \end{pmatrix}. \quad (4)$$

We can derive an expression for F_v in terms of the eigenvalues and eigenstates of $\hat{H}_v$ (see Supplemental Material [31]). The first term in Eq. (4) is chosen so that the photon density is ϕ^2. The results below are then obtained by minimizing over the variational parameters $(\phi, \nu_{\mathbf{q}}, \eta^e_{\mathbf{k}}, \eta^h_{\mathbf{k}}, \Delta_{\mathbf{k}}, \mathbf{Q})$. Because this ansatz contains only pairing of fermions and displacement of bosons, it is equivalent to mean-field theory approaches. A challenge for future work is to include higher order correlations such as those responsible for trions or attractive polarons [37,38]. Such correlations however can be suppressed by considering a spin polarized gas.

Pairing phases.—Previous work [11] explored the ground state phase diagram of Eq. (1) in the absence of coupling to photons, using the grand canonical ensemble with a charge imbalance chemical potential μ_c ($\hat{H} \to \hat{H} - \mu_c S\hat{n}_c$) in place of a realistic electrostatic energy [39]. It predicted first order phase transitions between a balanced condensate with $\langle \hat{n}_c \rangle = 0$ and an imbalanced $\langle \hat{n}_c \rangle \neq 0$ anisotropic FFLO condensate with nonzero center-of-mass momentum $Q \sim |\langle \hat{n}_e \rangle^{1/2} - \langle \hat{n}_h \rangle^{1/2}|$. When applied to the exciton only problem, our more realistic description of electrostatics shows that the transition between a $\mathbf{Q} = \mathbf{0}$ condensate and the FFLO state is continuous as a function of gate voltage [31].

When the balanced condensate is coupled to photons, it becomes a polaritonic state, with exciton-photon coherence, further lowering its energy. In contrast, coupling to photons has little influence on the FF state because excitons with center-of-mass momentum $\mathbf{Q}$ couple to photons at the same momentum, and the small photon mass places these far off resonance. The photon fraction in the FF state is therefore very small, and we thus refer to this state as dark. Coupling to photons therefore favors states with a small center-of-mass momentum. Numerical minimization indeed reveals that, at moderate imbalance, coupling to photons yields a bright polaritonic condensate state with $\mathbf{Q}$ small but nonzero. Surprisingly, this state accommodates excess carriers by spontaneously breaking rotational and time-reversal symmetry. At larger imbalance, the expected FF phase is recovered (for the extreme imbalance case, see Ref. [40]).

Figure 2 shows how the electron momentum distribution changes with charge imbalance (corresponding cross sections also showing hole occupation and coherence are presented in [31]). Panel (a) shows the case with $n_0 = 0$, i.e., balanced populations. At small n_0 [panel (b)], the state

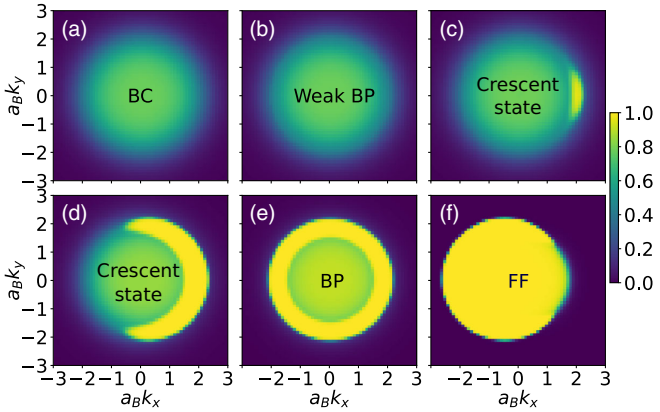

FIG. 2. Electron occupation $\langle \hat{e}^\dagger_{\mathbf{Q}/2+\mathbf{k}} \hat{e}_{\mathbf{Q}/2+\mathbf{k}} \rangle$ for various imbalance values $n_0 a_B^2$: (a) 0, (b) 6.25×10^{-3}, (c) 1.875×10^{-2}, (d) 0.125, (e) 0.1875, (f) 0.25. Labels on each panel indicate the phases as described in the text. The values of Qa_B are (c) 0.5×10^{-6}, (d) 0.5×10^{-5}, (f) 1.05, and zero for panels (a),(b),(e). Other parameters are as in Fig. 1.

maintains $\mathbf{Q} = \mathbf{0}$ to take optimal advantage of the photon-mediated electron-hole coupling. In the zero temperature limit, accommodating extra charges requires forming a Fermi surface, enclosing regions of momentum space in which both valence and conduction band states are occupied. At low charge imbalance, the Fermi sea forms a ring at the outer edge of the region of paired electrons. We will refer to the state at low carrier densities as a "weak breached pair" (WBP) state as it is reminiscent of the two-Fermi surface breached pair state described in Ref. [16]. In contrast to the fully breached pair, the coherence in Fig. 2(b) is only weakly suppressed in the region where extra electrons exist because the temperature is comparable to the conduction band Fermi energy. For intermediate n_0 [panels (c),(d)], we find a surprising broken rotational symmetry anisotropic state with $0 < Q \ll |\langle \hat{n}_e \rangle^{1/2} - \langle \hat{n}_h \rangle^{1/2}|$. Here, the unpaired carriers are contained in a Fermi pocket with a crescent shape on the edge of the otherwise circular electron distribution; hence we refer to it as the crescent state (CS). As n_0 increases further, the crescent extends in angle. Eventually it is replaced by a filled annulus [panel (e)], equivalent to the breached pair (BP) state of Ref. [16]. Finally, at large enough n_0, one recovers the dark FF state. Further increasing n_0 brings the system to a normal state (not shown). This sequence occurs at high excitation density $\hat{n}_{\mathrm{ex}}$. At low $\hat{n}_{\mathrm{ex}}$ (not shown) the BP state is replaced by a Sarma state where excess particles occupy a single isotropic Fermi surface [15], matching the extreme imbalance limit [40].

Phase diagram.—Figure 3 illustrates how the minimum free energy state evolves with target charge density and temperature by plotting charge imbalance, electronic excitation density, photon density, and anisotropy $\mathcal{A} \equiv \sum_{\mathbf{k}} |\hat{\mathbf{k}} \cdot \hat{\mathbf{Q}}| \langle \hat{e}^\dagger_{\mathbf{Q}/2+\mathbf{k}} \hat{e}_{\mathbf{Q}/2+\mathbf{k}} \rangle / \sum_{\mathbf{k}} \langle \hat{e}^\dagger_{\mathbf{Q}/2+\mathbf{k}} \hat{e}_{\mathbf{Q}/2+\mathbf{k}} \rangle$. This figure demonstrates that the CS persists over a wide

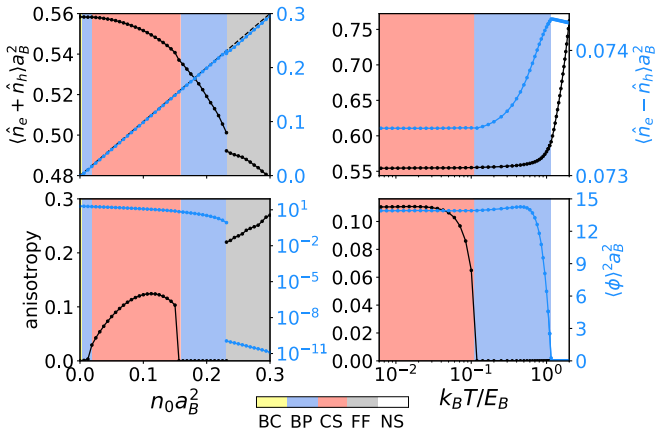

FIG. 3. Evolution of state with target charge density n_0 at $k_B T = 0.04 E_B$ (left) and with temperature T at $n_0 a_B^2 = 0.075$ (right); other parameters as in Fig. 1. Top panels show excitonic density (black; left axis) and charge imbalance (blue; right axis). The dashed blue line shows n_0. Bottom panels show anisotropy (black; left axis) and photon density $\phi^2 a_B^2$ (blue; right axis).

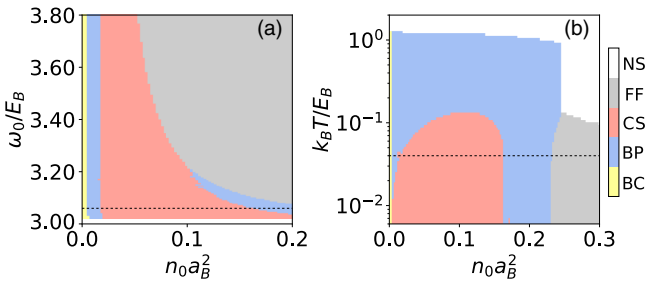

FIG. 4. Phase diagrams. (a) as a function of charge density n_0 and photon cutoff frequency ω_0 at $k_B T = 0.04 E_B$. (b) as a function of charge density n_0 and temperature T at $\omega_0 = 3.06 E_B$. The dashed lines indicate $\omega_0 = 3.06 E_B$ (left) and $k_B T = 0.04 E_B$, respectively. All other parameters are as in Fig. 1.

temperature range before being replaced by the WBP (isotropic) state. From this figure we see that most transitions, other than those into and out of the BP state, are continuous.

The quantities plotted in Fig. 3 allow us to classify phases and extract the phase diagrams in Fig. 4. Because the BP and CS have significant photon fractions, the small photon mass should allow them to survive to high temperature even when the collective fluctuations (absent in our mean-field theory) are included [41]. In contrast, the larger excitonic mass restricts the excitonic FF state to low temperatures. The survival of the CS up to $k_B T \simeq 0.1 E_B$ also suggests this state can survive the broadening introduced by cavity loss, which varies between $10^{-4} E_B$ and $10^{-2} E_B$ depending on material.

Since the CS is stabilized by the matter-light coupling, an experimentally accessible way to alter its robustness is by changing the photon cutoff frequency, ω_0, e.g., using a wedge cavity. When the photon is detuned far above the exciton energy, the cavity has little effect and excitonic results should be recovered. Figure 4(a) shows such a phase diagram as a function of n_0 and ω_0. Because physical states require $\mu_{ex} < \omega_0$, the lower boundary of this phase diagram cuts off just above this limit. As expected the CS becomes less prominent with increasing ω_0, although a narrow stability interval persists up to large detunings. In all the results we present here, $\mu_{\rm ex} - E_G = E_B$, providing an excitation density in the BEC-BCS crossover regime. Recent experiments suggest that this regime is attainable [42]. We avoid the lower excitation density BEC regime as it is known that, at finite temperature, fluctuation corrections to mean-field theory are important here [41,43].

Crescent state properties.—The CS is anisotropic with the same symmetries as the FF state but, in distinction, has a significant photon fraction and a qualitatively smaller pairing momentum. Because of its anisotropy, it is not immediately clear whether it has zero net current as expected by Bloch's theorem [44]. An explicit calculation shows that the CS has a nonzero excitonic current (electron current plus hole current) that is balanced by an equal and opposite photon current, i.e., a counterflow condensate state, generated by a shift in the condensate pair momentum from $\mathbf{Q} = \mathbf{0}$ to $\mathbf{Q}_{\rm min} \neq 0$ [45]. The momentum shift balances matter energy gain against photon kinetic energy cost. Since the shift is small enough to leave the electron and hole distributions almost unchanged, we can approximate $\mathbf{Q}_{\rm min} \simeq (m_{ph}/|\phi|^2)(\sum_{\mathbf{k}} \mathbf{k}[\langle \hat{e}^\dagger_{\mathbf{k}} \hat{e}_{\mathbf{k}} \rangle / m_e + \langle \hat{h}^\dagger_{\mathbf{k}} \hat{h}_{\mathbf{k}} \rangle / m_h])$, i.e., $|\mathbf{Q}_{\rm min}|$ is parametrically small due to the small photon to electron mass ratio. Indeed, as noted in the caption of Fig. 2, our numerical results for $|\mathbf{Q}_{\rm min}|$ in the CS are orders of magnitude smaller than in the FF state.

Since Bloch's theorem [44] can be generalized to a coupled photon-matter system, we expect that the charge current (electron current minus hole current) also vanishes. In our numerical calculations, we find that this cancellation is imperfect but ascribe the nonzero numerical result to the UV matter-light coupling cutoff κ discussed previously. In Ref. [31], we show that this charge current vanishes as the UV cutoff diverges.

The CS is a metal with a single Fermi surface for unpaired electrons, and we expect that it will exhibit metallic transport properties. The anisotropic Fermi surface in Fig. 2 implies anisotropic electrical transport with larger conduction along the thin direction of the crescent, i.e., in the direction parallel to $\mathbf{Q}$, that can be used to identify the CS experimentally. Any weak perturbation, for example weak resonant excitation or spatial anisotropy of a weak polariton confinement landscape, can be used to control the sense of anisotropy, possibly *in situ*. Also, since the CS breaks inversion symmetry, nonlinear ac response is also expected to exhibit rectification. The broken inversion should also enable optical signatures of second harmonic generation.

Notably, both strong matter-light coupling and long-range Coulomb interactions are required to stabilize the CS. While the photon promotes $\mathbf{Q} \approx \mathbf{0}$ pairing, it is the long-range Coulomb interaction that favors anisotropy. Indeed, screening the Coulomb interaction eventually leads to a continuous transition from the anisotropic CS to an isotropic state (see Ref. [31]). We therefore expect that our mean-field calculations overestimate the stability range of the CS. It is known that for the FF state (which has the same symmetries as the CS) fluctuations destroy long-range order [46,47] but some residual order survives [48]. Understanding the scales over which the CS order persists, and the consequences for charge transport, is a challenge for future work.

Conclusions.—Since the CS and BP states are polaritonic, they are expected to survive to high temperatures and should therefore be accessible in current experiments involving doped quantum wells [49–54] or 2D materials in cavities [37,55,56]. Our work focuses on the small imbalance regime where we are most confident about our conclusions. At high doping, one instead may consider Fermi-edge (Mahan) excitons (see e.g., [38,57] and references therein). Open questions include how the states we consider here connect to these Fermi-edge states, the effects of electronic screening in a charge doped system, and practical treatments that go beyond mean-field theory.

The research data supporting this publication can be accessed at [58].

We acknowledge helpful discussions with J. Levinsen, M. Parish, P. Pieri, and D. Golez. The Flatiron Institute is a division of the Simons Foundation. A. S. acknowledges support from the Engineering and Physical Sciences Research Council (EPSRC) CM-CDT (EP/L015110/1) and a travel award from the Scottish Universities Physics Alliance. A. S., A. H. M., and J. K. acknowledge financial support from a Royal Society International Exchange Award No. IES\R2\170213. F. M. M. acknowledges financial support from the Spanish Ministry of Science and Innovation through the Project No. MAT2017-83772-R and the María de Maeztu Programme for Units of Excellence in R&D (CEX2018-000805-M). J. K. acknowledges financial support from EPSRC program "Hybrid Polaritonics" (EP/M025330/1). A. H. M. acknowledges support from Army Research Office (ARO) Grant No. W911NF-17-1-0312 (MURI). This work was performed in part at Aspen Center for Physics, which is supported by National Science Foundation Grant No. PHY-1607611 and partially supported by a grant from the Simons Foundation.

[1] L. Keldysh and Y. V. Kopaev, Possible instability of the semimetal state with respect to Coulomb interaction, Sov. Phys. Solid State **6**, 2219 (1965) [Fiz. Tverd Tela **6**, 2791 (1964)].

[2] C. Comte and P. Nozières, Exciton Bose condensation: The ground state of an electron-hole gas I. Mean field description of a simplified model, J. Phys. **43**, 1069 (1982).

[3] A. A. High, J. R. Leonard, A. T. Hammack, M. M. Fogler, L. V. Butov, A. V. Kavokin, K. L. Campman, and A. C. Gossard, Spontaneous coherence in a cold exciton gas, Nature (London) **483**, 584 (2012).

[4] M. Fogler, L. Butov, and K. Novoselov, High-temperature superfluidity with indirect excitons in van der Waals heterostructures, Nat. Commun. **5**, 4555 (2014).

[5] Z. Wang, D. A. Rhodes, K. Watanabe, T. Taniguchi, J. C. Hone, J. Shan, and K. F. Mak, Evidence of high-temperature exciton condensation in two-dimensional atomic double layers, Nature (London) **574**, 76 (2019).

[6] P. Pieri, D. Neilson, and G. C. Strinati, Effects of density imbalance on the BCS-BEC crossover in semiconductor electron-hole bilayers, Phys. Rev. B **75**, 113301 (2007).

[7] A. L. Subası, P. Pieri, G. Senatore, and B. Tanatar, Stability of Sarma phases in density imbalanced electron-hole bilayer systems, Phys. Rev. B **81**, 075436 (2010).

[8] K. Yamashita, K. Asano, and T. Ohashi, Quantum condensation in electronHole bilayers with density imbalance, J. Phys. Soc. Jpn. **79**, 033001 (2010).

[9] M. M. Parish, F. M. Marchetti, and P. B. Littlewood, Supersolidity in electron-hole bilayers with a large density imbalance, Europhys. Lett. **95**, 27007 (2011).

[10] D. Neilson, A. Perali, and A. R. Hamilton, Excitonic superfluidity and screening in electron-hole bilayer systems, Phys. Rev. B **89**, 060502(R) (2014).

[11] J. R. Varley and D. K. K. Lee, Structure of exciton condensates in imbalanced electron-hole bilayers, Phys. Rev. B **94**, 174519 (2016).

[12] P. Fulde and R. A. Ferrell, Superconductivity in a strong spin-exchange field, Phys. Rev. **135**, A550 (1964).

[13] A. I. Larkin and Y. N. Ovchinnikov, Nonuniform state of superconductors, Zh. Eksp. Teor. Fiz. **47**, 1136 (1964) [Sov. Phys. JETP **20**, 762 (1965)].

[14] D. E. Sheehy and L. Radzihovsky, BEC–BCS crossover, phase transitions and phase separation in polarized resonantly-paired superfluids, Ann. Phys. (Amsterdam) **322**, 1790 (2007).

[15] G. Sarma, On the influence of a uniform exchange field acting on the spins of the conduction electrons in a superconductor, J. Phys. Chem. Solids **24**, 1029 (1963).

[16] M. M. Forbes, E. Gubankova, W. V. Liu, and F. Wilczek, Stability Criteria for Breached-Pair Superfluidity, Phys. Rev. Lett. **94**, 017001 (2005).

[17] M. W. Zwierlein, A. Schirotzek, C. H. Schunck, and W. Ketterle, Fermionic superfluidity with imbalanced spin populations, Science **311**, 492 (2006).

[18] G. B. Partridge, W. Li, R. I. Kamar, Y.-a. Liao, and R. G. Hulet, Pairing and phase separation in a polarized Fermi gas, Science **311**, 503 (2006).

[19] Y. Shin, M. W. Zwierlein, C. H. Schunck, A. Schirotzek, and W. Ketterle, Observation of Phase Separation in a Strongly Interacting Imbalanced Fermi Gas, Phys. Rev. Lett. **97**, 030401 (2006).

[20] J. Kasprzak, M. Richard, S. Kundermann, A. Baas, P. Jeambrun, J. M. J. Keeling, F. M. Marchetti, M. H. Szymańska,

R. André, J. L. Staehli, V. Savona, P. B. Littlewood, B. Deveaud, and L. S. Dang, Bose-Einstein condensation of exciton polaritons, Nature (London) **443**, 409 (2006).
[21] R. Balili, V. Hartwell, D. Snoke, L. Pfeiffer, and K. West, Bose-Einstein condensation of microcavity polaritons in a trap, Science **316**, 1007 (2007).
[22] C. Weisbuch, M. Nishioka, A. Ishikawa, and Y. Arakawa, Observation of the Coupled Exciton-Photon Mode Splitting in a Semiconductor Quantum Microcavity, Phys. Rev. Lett. **69**, 3314 (1992).
[23] I. Carusotto and C. Ciuti, Quantum fluids of light, Rev. Mod. Phys. **85**, 299 (2013).
[24] S. Takada and T. Izuyama, Superconductivity in a Molecular Field. I, Prog. Theor. Phys. **41**, 635 (1969).
[25] S. Giorgini, L. P. Pitaevskii, and S. Stringari, Theory of ultracold atomic Fermi gases, Rev. Mod. Phys. **80**, 1215 (2008).
[26] T. Byrnes, T. Horikiri, N. Ishida, and Y. Yamamoto, BCS Wave-Function Approach to the BEC-BCS Crossover of Exciton-Polariton Condensates, Phys. Rev. Lett. **105**, 186402 (2010).
[27] F. Xue, F. Wu, M. Xie, J.-J. Su, and A. H. MacDonald, Microscopic theory of equilibrium polariton condensates, Phys. Rev. B **94**, 235302 (2016).
[28] K. Kamide and T. Ogawa, What Determines the Wave Function of Electron-Hole Pairs in Polariton Condensates?, Phys. Rev. Lett. **105**, 056401 (2010).
[29] K. Kamide and T. Ogawa, Ground-state properties of microcavity polariton condensates at arbitrary excitation density, Phys. Rev. B **83**, 165319 (2011).
[30] J. Levinsen, G. Li, and M. M. Parish, Microscopic description of exciton-polaritons in microcavities, Phys. Rev. Research **1**, 033120 (2019).
[31] See Supplemental Material at http://link.aps.org/supplemental/10.1103/PhysRevLett.125.067405 for the explicit forms of the variational free energy, further illustrations of the evolution of the state with temperature and density, and discussions of the order of the phase transitions, gauge invariance, behavior in the limit of no photon coupling, the effects of screening and mass imbalance, and numerical methods from Ref. [32].
[32] P. Virtanen *et al.* (SciPy 1.0 Contributors), SciPy 1.0–fundamental algorithms for scientific computing in PYTHON, Nat. Methods **17**, 261 (2020).
[33] G. M. Andolina, F. M. D. Pellegrino, V. Giovannetti, A. H. MacDonald, and M. Polini, Cavity quantum electrodynamics of strongly correlated electron systems: A no-go theorem for photon condensation, Phys. Rev. B **100**, 121109(R) (2019).
[34] K. Rzażewski, K. Wódkiewicz, and W. Żakowicz, Phase Transitions, Two-Level Atoms, and the A^2 term, Phys. Rev. Lett **35**, 432 (1975).
[35] P. R. Eastham and P. B. Littlewood, Bose condensation of cavity polaritons beyond the linear regieme: The thermal equilibrium of a model microcavity, Phys. Rev. B **64**, 235101 (2001).
[36] H. Kleinert, *Path Integrals in Quantum Mechanics, Statistics, Polymer Physics, and Financial Markets*, (World scientific, Singapore, 2009).
[37] M. Sidler, P. Back, O. Cotlet, A. Srivastava, T. Fink, M. Kroner, E. Demler, and A. Imamoglu, Fermi polaron-polaritons in charge-tunable atomically thin semiconductors, Nat. Phys. **13**, 255 (2017).
[38] D. Pimenov, J. von Delft, L. Glazman, and M. Goldstein, Fermi-edge exciton-polaritons in doped semiconductor microcavities with finite hole mass, Phys. Rev. B **96**, 155310 (2017).
[39] Reference [11] however neglects intraspecies interactions which may affect its conclusions, see [7].
[40] A. Tiene, J. Levinsen, M. M. Parish, A. H. MacDonald, J. Keeling, and F. M. Marchetti, Extremely imbalanced two-dimensional electron-hole-photon systems, Phys. Rev. Research **2**, 023089 (2020).
[41] J. Keeling, P. R. Eastham, M. H. Szymanska, and P. B. Littlewood, BCS-BEC crossover in a system of microcavity polaritons, Phys. Rev. B **72**, 115320 (2005).
[42] J. Hu, Z. Wang, S. Kim, H. Deng, S. Brodbeck, C. Schneider, S. Höfling, N. H. Kwong, and R. Binder, Signatures of a Bardeen-Cooper-Schrieffer polariton laser, arXiv:1902.00142.
[43] P. Nozieres and S. Schmitt-Rink, Bose condensation in an attractive fermion gas: From weak to strong coupling superconductivity, J. Low Temp. Phys. **59**, 195 (1985).
[44] D. Bohm, Note on a theorem of Bloch concerning possible causes of superconductivity, Phys. Rev. **75**, 502 (1949).
[45] We note that in principle a similar statement, that a nonzero photon current and exciton current exist, but cancel at the optimum **Q**, also holds for the FF state. However as the FF state is almost entirely dark, this photonic current is negligible.
[46] H. Shimahara, Phase fluctuations and Kosterlitz-Thouless transition in two-dimensional Fulde-Ferrell-Larkin-Ovchinnikov superconductors, J. Phys. Soc. Jpn. **67**, 1872 (1998).
[47] Y. Ohashi, On the FuldeFerrell state in spatially isotropic superconductors, J. Phys. Soc. Jpn. **71**, 2625 (2002).
[48] L. Radzihovsky, Fluctuations and phase transitions in Larkin-Ovchinnikov liquid-crystal states of a population-imbalanced resonant Fermi gas, Phys. Rev. A **84**, 023611 (2011).
[49] T. Brunhes, R. André, A. Arnoult, J. Cibert, and A. Wasiela, Oscillator strength transfer from X to X^+ in a CdTe quantum-well microcavity, Phys. Rev. B **60**, 11568 (1999).
[50] R. Rapaport, E. Cohen, A. Ron, E. Linder, and L. N. Pfeiffer, Negatively charged polaritons in a semiconductor microcavity, Phys. Rev. B **63**, 235310 (2001).
[51] A. Qarry, R. Rapaport, G. Ramon, E. Cohen, A. Ron, and L. N. Pfeiffer, Polaritons in microcavities containing a two-dimensional electron gas, Semicond. Sci. Technol. **18**, S331 (2003).
[52] D. Bajoni, M. Perrin, P. Senellart, A. Lemaître, B. Sermage, and J. Bloch, Dynamics of microcavity polaritons in the presence of an electron gas, Phys. Rev. B **73**, 205344 (2006).
[53] A. Gabbay, Y. Preezant, E. Cohen, B. M. Ashkinadze, and L. N. Pfeiffer, Fermi Edge Polaritons in a Microcavity Containing a High Density Two-Dimensional Electron Gas, Phys. Rev. Lett. **99**, 157402 (2007).

[54] S. Smolka, W. Wuester, F. Haupt, S. Faelt, W. Wegscheider, and A. Imamoglu, Cavity quantum electrodynamics with many-body states of a two-dimensional electron gas, Science **346**, 332 (2014).

[55] B. Chakraborty, J. Gu, Z. Sun, M. Khatoniar, R. Bushati, A. L. Boehmke, R. Koots, and V. M. Menon, Control of strong light–matter interaction in monolayer WS_2 through electric field gating, Nano Lett. **18**, 6455 (2018).

[56] H. A. Fernandez, F. Withers, S. Russo, and W. L. Barnes, Electrically Tuneable Exciton-Polaritons through Free Electron Doping in Monolayer WS_2 microcavities, Adv. Opt. Mater. **7**, 1900484 (2019).

[57] G. Mahan, *Many-Particle Physics*, Physics of Solids and Liquids (Springer, New York, 2013).

[58] https://doi.org/10.17630/5268422e-fdc4-4b76-a11f-1ee5733b4f62.